

FINITE ELEMENT ANALYSIS OF THERMO-DIFFUSION AND DIFFUSION-THERMO EFFECTS ON COMBINED HEAT AND MASS TRANSFER FLOW OF VISCOUS, ELECTRICALLY CONDUCTING FLUID THROUGH A POROUS MEDIUM IN A VERTICAL CHANNEL

C. Sulochana¹ and Tayappa H.*²

¹*Professor, Dept. of Mathematics, Gulbarga University, Gulbarga, Karnataka, India.*

²*Assistant Professor of Mathematics, SSA Govt. First Grade College, Bellary, Karnataka, India.*

(Received On: 04-09-14; Revised & Accepted On: 26-09-14)

ABSTRACT

In this paper we study the effects of thermo-diffusion and diffusion-thermo on non-Darcy convective heat and mass transfer flow of a viscous, electrically conducting fluid through a porous medium in a vertical channel whose walls are maintained at constant temperature and concentration. The porous medium is assumed to be isotropic and homogeneous with constant porosity and effective thermal diffusivity. The thermo physical properties of the solid and fluid have been assumed to be constant except for the density variation in the body force term and the solid properties and the fluid are considered to be in the thermal equilibrium. The non-linear coupled equations have been solved by a finite element technique with three noded line segments. The rate of heat transfer reduces with Schmidt parameter in heating case and enhances in the cooling case at both the walls. The rate of mass transfer with respect to Soret parameter reduces in the heating case and enhances in the cooling case.

Key Words: Soret effect, Dufour effect, MHD, Porous medium, Vertical channel, Finite element technique.

1. INTRODUCTION

Non – Darcy effects on natural convection in porous media have received a great deal of attention in recent years because of the experiments conducted with several combinations of solids and fluids covering wide ranges of governing parameters which indicate that the experimental data for systems other than glass water at low Rayleigh numbers, do not agree with theoretical predictions based on the Darcy flow model. This divergence in the heat transfer results has been reviewed in detail in Cheng [5], Prasad *et al* [16] among others. Extensive effects are thus being made to include the inertia and viscous diffusion terms in the flow equations and to examine their effects in order to develop a reasonable accurate mathematical model for convective transport in porous media. The work of Vafai and Tien [21] was one of the early attempts to account for the boundary and inertia effects in the momentum equation for a porous

medium. They found that the momentum boundary layer thickness is of order of $\sqrt{\frac{k}{\epsilon}}$. Vafai and Thyagaraju [22]

presented analytical solutions for the velocity and temperature fields for the interface region using the Brinkman Forchheimer–extended Darcy equation. Detailed accounts of the recent efforts on non-Darcy convection have been recently reported in Tien and Hong [19], Prasad *et al* [16] and Kalidas and Prasad [9]. Here, we will restrict our discussion to the vertical cavity only. Poulikakos and Bejan [14] investigated the inertia effects through the inclusion of Forchheimer’s velocity squared term, and presented the boundary layer analysis for tall cavities. They also obtained numerical results for a few cases in order to verify the accuracy of their boundary layer analysis for tall cavities. Later, Prasad and Tuntomo [15] reported an extensive numerical work for a wide range of parameters and demonstrated that effects of Prandtl number remain almost unaltered while the dependence on the modified Grashof number Gr changes significantly with an increase in the Forchheimer number. This result in reversal of flow regimes from boundary layer to asymptotic to conduction as the contribution of the inertia term increases in comparison with that of the boundary term. They also reported a criterion for the Darcy flow limit.

Corresponding author: Tayappa H.*²

²*Assistant Professor of Mathematics, SSA Govt. First Grade College, Bellary, Karnataka, India.*

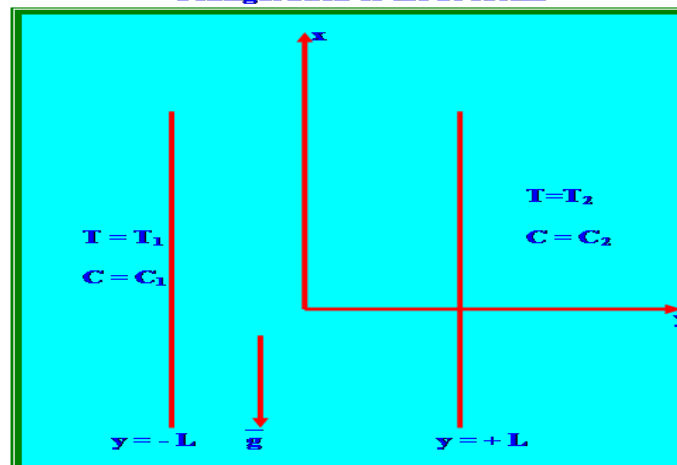
The Brinkman–Extended–Darcy modal was considered in Tong and Subramanian [20], Lauriat and Prasad [11] to examine the boundary effects on free convection in a vertical cavity. While Tong and Subramanian performed a Weber – type boundary layer analysis, Lauriat and Prasad solved the problem numerically for $A=1$ and 5 . It was shown that for a fixed modified Rayleigh number Ra , the Nusselt number decreases with an increase in the Darcy number, the reduction being larger at higher values of Ra . A scale analysis as well as the computational data also showed that the transport term $(\mathbf{v} \cdot \nabla) \mathbf{v}$ is of low order of magnitude compared to the diffusion plus buoyancy terms [11]. A numerical study based on the Forchheimer-Brinkman-Extended Darcy equation of motion has also been reported recently by Beckerman et al [4]. They demonstrated that the inclusion of both the inertia and boundary effects is important for convection in a rectangular packed – sphere cavity.

Also in all the above studies the thermal diffusion effect (known as Soret effect) has been neglected. This assumption is true when the concentration level is very low. The thermal diffusion effects for instance, has been utilized for isotropic separation and in mixtures between gases with very light molecular weight (H_2 , He) and the medium molecular weight (N_2 , air) the diffusion– thermo effects was found to be of a magnitude just it can not be neglected. In view of the importance of this diffusion– thermo effect, recently Jha and singh [7] studied the free convection and mass transfer flow in an infinite vertical plate moving impulsively in its own plane taking into account the Soret effect. Kafousias [8] studied the MHD free convection and mass transfer flow taking into account Soret effect. The analytical studies of Jha and singh and Kafousias [7, 8] were based on Laplace transform technique. Abdul Sattar and Alam [1] have considered an unsteady convection and mass transfer flow of viscous incompressible and electrically conducting fluid past a moving infinite vertical porous plate taking into the thermal diffusion effects. Similarity equations of the momentum energy and concentration equations are derived by introducing a time dependent length scale. Malasetty *et al* [13] have studied the effect of both the Soret coefficient and Dufour coefficient on the double diffusive convective with compensating horizontal thermal and solutal gradients.

The effects of radiation on MHD flow and heat transfer problem have become more important industrially. Many processes in engineering areas occur at high temperature and knowledge of radiation heat transfer becomes very important for the design of the pertinent equipment. Nuclear power plants, Gas turbines and various propulsion devices, for aircraft, missiles, satellites and space vehicles are examples of such engineering areas. Recently Bharathi [3] has studied thermo-diffusion effect on unsteady convective Heat and Mass transfer flow of a viscous fluid through a porous medium in vertical channel. Radiative flow plays a vital role in many industrial and environmental process e.g. heating and cooling chambers, fossil fuel combustion energy process, evaporation from larger open water reservoirs, astrophysical flows, solar power technology and space vehicle re-entry. Taneja *et al* [18] studied the effects of magnetic field on free convective flow through porous medium with radiation and variable permeability in the slip flow regime. Kumar *et al* [10] studied the effect of MHD free convection flow of viscous fluid past a porous vertical plate through non homogeneous porous medium with radiations and temperature gradient dependent heat source in slip flow regime. The effect of free convection flow with thermal radiation and mass transfer past a moving vertical porous plate was studied by Makinde [12]. Ayani *et al* [2] studied the effect of radiation on the laminar natural convection induced by a line source. Raphil [17] have discussed the effect of radiation and free convection flow through porous medium. MHD oscillating flow on free convection radiation through porous medium with constant suction velocity was investigated by El.Hakim [6].

Keeping the above application in view we made an attempt in this paper to study thermo-diffusion and diffusion-thermo effects on non-Darcy convective heat and Mass transfer flow of a viscous electrically conducting fluid through a porous medium in a vertical channel. The governing equations of flow, heat and mass transfer are solved by using Galerkin finite element analysis with three noded line segments. The velocity, temperature, concentration, the rate of Heat and Mass transfer are evaluated numerically for different variations of parameters.

Configuration of the Problem



2. FORMULATION OF THE PROBLEM

We consider a fully developed laminar convective heat and mass transfer flow of a viscous, electrically conducting fluid through a porous medium confined in a vertical channel bounded by flat walls. We choose a Cartesian co-ordinate system O(x,y,z) with x- axis in the vertical direction and y-axis normal to the walls. The walls are taken at $y = \pm L$. The walls are maintained at constant temperature and concentration. The temperature gradient in the flow field is sufficient to cause natural convection in the flow field. A constant axial pressure gradient is also imposed so that this resultant flow is a mixed convection flow. The porous medium is assumed to be isotropic and homogeneous with constant porosity and effective thermal diffusivity. The thermo physical properties of porous matrix are also assumed to be constant and Boussinesq approximation is invoked by confining the density variation to the buoyancy term. In the absence of any extraneous force flow is unidirectional along the x-axis which is assumed to be infinite.

The Brinkman-Forchheimer-extended Darcy equation which account for boundary inertia effects in the momentum equation is used to obtain the velocity field. Based on the above assumptions the governing equations in the vector form are

$$\nabla \cdot \bar{q} = 0 \quad (\text{Equation of continuity}) \quad (1)$$

$$\frac{\rho}{\delta} \frac{\partial \bar{q}}{\partial t} + \frac{\rho}{\delta^2} (\bar{q} \cdot \nabla) \bar{q} = -\nabla p + \rho g - \left(\frac{\sigma \mu_e^2 H_o^2}{\rho_o} \right) \bar{q} - \frac{\rho F}{\sqrt{k}} \bar{q} \cdot \bar{q} + \mu \nabla^2 \bar{q} \quad (\text{Equation of linear momentum}) \quad (2)$$

$$\rho C_p \left(\frac{\partial T}{\partial t} + (\bar{q} \cdot \nabla) T \right) = k_f \nabla^2 T + k_{12} \nabla^2 C \quad (\text{Equation of energy}) \quad (3)$$

$$\frac{\partial C}{\partial t} + (\bar{q} \cdot \nabla) C = D_1 \nabla^2 C - KC + k_{11} \nabla^2 T \quad (\text{Equation of diffusion}) \quad (4)$$

$$\rho - \rho_0 = -\beta \rho_0 (T - T_0) - \beta^* \rho_0 (C - C_0) \quad (\text{Equation of State}) \quad (5)$$

where $\bar{q} = (u, 0, 0)$ is the velocity, T, C are the temperature and Concentration, p is the pressure, ρ is the density of the fluid, g is the acceleration due gravity, C_p is the specific heat at constant pressure, μ is the coefficient of viscosity, k is the permeability of the porous medium, δ is the porosity of the medium, β is the coefficient of thermal expansion, k_f is the coefficient of thermal conductivity, F is a function that depends on the Reynolds number and the microstructure of porous medium, β^* is the volumetric coefficient of expansion with mass fraction concentration, K is the chemical reaction coefficient and D_1 is the chemical molecular diffusivity, k_{11} is the cross diffusivity. Here the thermo-physical properties of the solid and fluid have been assumed to be constant except for the density variation in the body force term (Boussinesq approximation) and the solid particles and the fluid are considered to be in the thermal equilibrium.

Since the flow is unidirectional, the continuity equation (1) reduces to

$$\frac{\partial u}{\partial x} = 0 \quad \text{where } u \text{ is the axial velocity implies } u = u(y)$$

The momentum, energy and diffusion equations in the scalar form reduces to

$$-\frac{\partial p}{\partial x} + \left(\frac{\mu}{\delta} \right) \frac{\partial^2 u}{\partial y^2} - \left(\frac{\sigma \mu_e^2 H_o^2}{\rho_o} \right) u - \frac{\rho \delta F}{\sqrt{k}} u^2 + \rho g = 0 \quad (6)$$

$$\rho_0 C_p u \frac{\partial T}{\partial x} = k_f \frac{\partial^2 T}{\partial y^2} + k_{12} \frac{\partial^2 C}{\partial y^2} \quad (7)$$

$$u \frac{\partial C}{\partial x} = D_1 \frac{\partial^2 C}{\partial y^2} + k_{11} \frac{\partial^2 T}{\partial y^2} \quad (8)$$

The boundary conditions are

$$\begin{aligned} u = 0, \quad T = T_1 \quad C = C_1 \quad \text{on } y = -L \\ u = 0, \quad T = T_2 \quad C = C_2 \quad \text{on } y = +L \end{aligned} \quad (9)$$

The axial temperature and concentration gradients $\frac{\partial T}{\partial x}$ & $\frac{\partial C}{\partial x}$ are assumed to be constant, say A & B respectively.

We define the following non-dimensional variables as

$$u' = \frac{u}{(v/L)}, (x', y') = (x, y)/L, \quad p' = \frac{p\delta}{(\rho v^2/L^2)} \quad (10)$$

$$\theta = \frac{T-T_2}{T_1-T_2}, \quad C' = \frac{C-C_2}{C_1-C_2}$$

Introducing these non-dimensional variables, the governing equations in the dimensionless form reduce to (on dropping the dashes)

$$\frac{d^2 u}{dy^2} = \pi + \delta(M_1^2)u - \delta G(\theta + NC) - \delta^2 \Delta u^2 \quad (11)$$

$$\frac{d^2 \theta}{dy^2} = (PN_T)u - Du \frac{d^2 C}{dy^2} \quad (12)$$

$$\frac{d^2 C}{dy^2} = (Sc N_c)u + \frac{ScSo}{N} \frac{d^2 \theta}{dy^2} \quad (13)$$

where

$$\Delta = FD^{-1/2} \quad (\text{Inertia or Forchhimer parameter})$$

$$G = \frac{\beta g(T_1 - T_2)L^3}{v^2} \quad (\text{Grashof Number})$$

$$M^2 = \frac{\sigma \mu_e^2 H_o^2 L^2}{v^2} \quad (\text{Hartmann Number})$$

$$Sc = \frac{\nu}{D_1} \quad (\text{Schmidt number})$$

$$N = \frac{\beta^*(C_1 - C_2)}{\beta(T_1 - T_2)} \quad (\text{Buoyancy ratio})$$

$$P = \frac{\mu C_p}{k_f} \quad (\text{Prandtl Number})$$

$$N_T = \frac{AL}{(T_1 - T_2)} \quad (\text{Non-dimensional temperature gradient})$$

$$N_c = \frac{BL}{(C_1 - C_2)} \quad (\text{Non-dimensional concentration gradient})$$

$$S_0 = \frac{k_{11}\Delta T}{v\Delta T} \quad (\text{Soret parameter})$$

$$Du = \frac{k_{12}\Delta C}{k_f \Delta t} \quad (\text{Dufour parameter})$$

The corresponding boundary conditions are

$$u = 0, \quad \theta = 1, \quad C = 1 \quad \text{on } y = -1$$

$$u = 0, \quad \theta = 0, \quad C = 0 \quad \text{on } y = +1 \quad (14)$$

3. FINITE ELEMENT ANALYSIS

To solve these differential equations with the corresponding boundary conditions, we assume that if u^i, θ^i, c^i are the approximations of u, θ and C we define the errors (residual) E_u^i, E_θ^i, E_c^i as

$$E_u^i = \frac{d}{d\eta} \left(\frac{du^i}{d\eta} \right) - M_1^2 u^i + \delta^2 A(u^i)^2 - \delta G(\theta^i + NC^i) \quad (15)$$

$$E_c^i = \frac{d}{dy} \left(\frac{dC^i}{dy} \right) + \frac{ScSo}{N} \frac{d}{dy} \left(\frac{d\theta^i}{dy} \right) - ScN_c u^i \quad (16)$$

$$E_\theta^i = \frac{d}{dy} \left(\frac{d\theta^i}{dy} \right) - P_1 N_T u^i + Du N_2 \frac{d}{dy} \left(\frac{d^i}{dy} \right) \quad (17)$$

where

$$\left. \begin{aligned} u^i &= \sum_{k=1}^3 u_k \psi_k \\ C^i &= \sum_{k=1}^3 C_k \psi_k \\ \theta^i &= \sum_{k=1}^3 \theta_k \psi_k \end{aligned} \right\} \quad (18)$$

These errors are orthogonal to the weight function over the domain of e^i under Galerkin finite element technique we choose the approximation functions as the weight function. Multiply both sides of the equations (15-17) by the weight function i.e. each of the approximation function ψ_j^i and integrate over the typical three noded linear element

(η_e, η_{e+1}) we obtain

$$\int_{\eta_e}^{\eta_{e+1}} E_u^i \psi_j^i dy = 0 \quad (i = 1, 2, 3, 4,) \quad (19)$$

$$\int_{\eta_e}^{\eta_{e+1}} E_c^i \psi_j^i dy = 0 \quad (i = 1, 2, 3, 4,) \quad (20)$$

$$\int_{\eta_e}^{\eta_{e+1}} E_\theta^i \psi_j^i dy = 0 \quad (i = 1, 2, 3, 4,) \quad (21)$$

where

$$\int_{\eta_e}^{\eta_{e+1}} \left(\frac{d}{d\eta} \left(\frac{du^i}{d\eta} \right) - M_1^2 u^i + \delta^2 A (u^i)^2 - \delta G (\theta^i + NC^i) \right) \psi_j^i dy = 0 \quad (22)$$

$$\int_{\eta_e}^{\eta_{e+1}} \left(\frac{d}{dy} \left(\frac{dC^i}{dy} \right) + \frac{ScSo}{N} \frac{d}{dy} \left(\frac{d\theta^i}{dy} \right) - ScN_c u^i \right) \psi_j^i dy = 0 \quad (23)$$

$$\int_{\eta_e}^{\eta_{e+1}} \left(\frac{d}{dy} \left(\frac{d\theta^i}{dy} \right) - P_1 N_T u^i + Du \frac{d}{dy} \left(\frac{d^i}{dy} \right) \right) \psi_j^i dy = 0 \quad (24)$$

Following the Galerkin weighted residual method and integration by parts method to the equations (22) – (24) we obtain

$$\int_{\eta_e}^{\eta_{e+1}} \frac{d\Psi_j^i}{dy} \frac{du^i}{dy} dy - \delta M_1^2 \int_{\eta_e}^{\eta_{e+1}} u^i \Psi_j^i dy + \delta^2 A \int_{\eta_e}^{\eta_{e+1}} (u^i)^2 \Psi_j^i dy - \delta G \int_{\eta_e}^{\eta_{e+1}} (\theta^i + NC^i) \Psi_j^i dy = Q_{1,j} + Q_{2,j} \quad (25)$$

where $-Q_{1,j} = \Psi_j(\eta_e) \frac{du^i}{d\eta}(\eta_e)$

$$Q_{2,j} = \Psi_j(\eta_{e+1}) \frac{du^i}{d\eta}(\eta_{e+1})$$

$$\int_{\eta_e}^{\eta_{e+1}} \frac{d\Psi_j^i}{dy} \left(\frac{dC^i}{dy} \right) dy - \frac{ScSo}{N} \int_{\eta_e}^{\eta_{e+1}} \frac{d\Psi_j^i}{dy} \left(\frac{d\theta^i}{dy} \right) \Psi_j^i dy - ScN_c \int_{\eta_e}^{\eta_{e+1}} u^i \Psi_j^i dy = R_{1,j} + R_{2,j} \quad (26)$$

$$\text{where } -R_{1,j} = \Psi_j(\eta_e) \frac{dC^i}{dy}(\eta_e) + \frac{ScSo}{N} \Psi_j(\eta_e) \frac{d\theta^i}{dy}(\eta_e)$$

$$R_{2,j} = \Psi_j(\eta_{e+1}) \left(\frac{dC^i}{dy}(\eta_{e+1}) + \frac{ScSo}{N} \frac{d\theta^i}{dy}(\eta_{e+1}) \right)$$

$$\int_{\eta_e}^{\eta_{e+1}} \frac{d\Psi_j^i}{dy} \frac{d\theta^i}{dy} dy - P_1 N_T \int_{\eta_e}^{\eta_{e+1}} u^i \Psi_j^i dy + Du N_2 \int_{\eta_e}^{\eta_{e+1}} \frac{d\Psi_j^i}{dy} \left(\frac{dC^i}{dy} \right) \Psi_j^i dy = S_{1,j} + S_{2,j} \quad (27)$$

$$\text{where } -S_{1,j} = \Psi_j(\eta_e) \frac{d\theta^i}{dy}(\eta_e) + Du N_2 \Psi_j(\eta_e) \frac{dC^i}{dy}(\eta_e)$$

$$S_{2,j} = \Psi_j(\eta_{e+1}) \frac{d\theta^i}{dy}(\eta_{e+1}) + Du N_2 \Psi_j(\eta_{e+1}) \frac{dC^i}{dy}(\eta_{e+1})$$

Making use of equations (18) we can write above equations as

$$\begin{aligned} \sum_{k=1}^3 u_k \int_{\eta_e}^{\eta_{e+1}} \frac{d\Psi_j^i}{dy} \frac{d\Psi_k}{dy} dy - \sum_{k=1}^3 \delta M_1^2 u_k \int_{\eta_e}^{\eta_{e+1}} \Psi_j^i \Psi_k dy - \delta G \left(\sum_{k=1}^3 \theta_k \int_{\eta_e}^{\eta_{e+1}} \Psi_j^i \Psi_k dy + NC_k \sum_{k=1}^3 \Psi_j^i \Psi_k dy \right. \\ \left. + \delta^2 A \sum_{k=1}^3 u_k^2 \int_{\eta_e}^{\eta_{e+1}} \left(\frac{d\Psi_k}{d\eta} \right)^2 \Psi_j^i dy \right) = Q_{1,j} + Q_{2,j} \end{aligned} \quad (28)$$

$$\sum_{k=1}^3 C_k \int_{\eta_e}^{\eta_{e+1}} \frac{d\Psi_j^i}{dy} \frac{d\Psi_k}{dy} dy - ScN_c \sum_{k=1}^3 C_k \int_{\eta_e}^{\eta_{e+1}} \Psi_j^i \Psi_k dy + \frac{ScSo}{N} \sum_{k=1}^3 \theta_k \int_{\eta_e}^{\eta_{e+1}} \frac{d\Psi_j^i}{dy} \frac{d\Psi_k}{dy} dy = R_{1,j} + R_{2,j} \quad (29)$$

$$\sum_{k=1}^3 \theta_k \int_{\eta_e}^{\eta_{e+1}} \frac{d\Psi_j^i}{dy} \frac{d\Psi_k}{dy} dy - PN_T \sum_{k=1}^3 u_k \int_{\eta_e}^{\eta_{e+1}} \Psi_k \Psi_j^i dy + Du \sum_{k=1}^3 C_k \int_{\eta_e}^{\eta_{e+1}} \frac{d\Psi_j^i}{dy} \frac{d\Psi_k}{dy} dy = S_{1,j} + S_{2,j} \quad (30)$$

Choosing different Ψ_j^i 's corresponding to each element η_e in the equation (28) yields a local stiffness matrix of order 3×3 in the form

$$(f_{i,j}^k)(u_i^k) - \delta G(g_{i,j}^k)(\theta_i^k + NC_i^k) + \delta D^{-1}(m_{i,j}^k)(u_i^k) + \delta^2 A(n_{i,j}^k)(u_{i,j}^k) = (Q_{i,j}^k) + (Q_{2,j}^k) \quad (31)$$

Likewise the equation (29) & (30) gives rise to stiffness matrices

$$(e_{i,j}^k)(C_i^k) + \frac{ScSo}{N}(t_{ij}^k)(\theta_i^k) - PN_C(m_{i,j}^k)(u_i^k) = R_{1,j}^k + R_{2,j}^k \quad (32)$$

$$(l_{ij}^k)(\theta_i^k) - P_r N_T(t_{ij}^k)(\theta_i^k) = S_{1,j}^k + S_{2,j}^k \quad (33)$$

where

$(f_{i,j}^k), (g_{i,j}^k), (m_{i,j}^k), (n_{i,j}^k), (e_{i,j}^k), (t_{ij}^k)$ are 3×3 matrices and $(Q_{2,j}^k), (Q_{1,j}^k), (R_{2,j}^k), (R_{1,j}^k), (S_{2,j}^k)$ and $(S_{1,j}^k)$ are 3×1 column matrices and such stiffness matrices (3.17) – (3.19) in terms of local nodes in each element are assembled using inter element continuity and equilibrium conditions to obtain the coupled global matrices in terms of the global nodal values of u , θ & C . In case we choose n -quadratic elements then the global matrices are of order $2n+1$. The ultimate coupled global matrices are solved to determine the unknown global nodal values of the velocity, temperature and concentration in fluid region. In solving these global matrices an iteration procedure has been adopted to include the boundary and effects in the porous region.

4. STIFFNESS MATRICES

The global matrix for θ is

$$A_3 X_3 = B_3 \quad (34)$$

The global matrix for N is

$$A_4 X_4 = B_4 \quad (35)$$

The global matrix u is

$$A_5 X_5 = B_5 \quad (36)$$

In fact, the non-linear term arises in the modified Brinkman linear momentum equation (22) of the porous medium. The iteration procedure in taking the global matrices as follows. We split the square term into a product term and keeping one of them say u_i 's under integration, the other is expanded in terms of local nodal values as in (18), resulting in the corresponding coefficient matrix (n_{ij}^k) 's in (31), whose coefficients involve the unknown u_i 's. To evaluate (32), to begin with choose the initial global nodal values of u_i 's as zeros in the zeroth approximation. We evaluate u_i 's, θ_i 's and C_i 's in the usual procedure mentioned earlier. Later choosing these values of u_i 's as first order approximation calculate θ_i 's, C_i 's. In the second iteration, we substitute for u_i 's the first order approximation of u_i 's and the first approximation of θ_i 's and C_i 's obtain second order approximation. This procedure is repeated till the consecutive values of u_i 's, θ_i 's and C_i 's differ by a preassigned percentage. For computational purpose we choose five elements in flow region.

5. SHEAR STRESS, NUSSELT NUMBER AND SHERWOOD NUMBER

The shear stress on the boundaries $y = \pm 1$ in the non-dimensional form is

$$\tau_{y=\pm 1} = \left(\frac{du}{dy} \right)_{y=\pm 1}$$

The rate of heat transfer (Nusselt Number) is given by

$$Nu_{y=\pm 1} = \left(\frac{d\theta}{dy} \right)_{y=\pm 1}$$

The rate of mass transfer (Sherwood Number) is given by

$$Sh_{y=\pm 1} = \left(\frac{dC}{dy} \right)_{y=\pm 1}$$

6. DISCUSSION OF RESULTS

In this analysis we discuss the combined influence of Soret and Dufour effects on Convective heat and mass transfer flow of a viscous electrically conducting fluid through a porous medium in a vertical channel whose walls are maintained at constant temperature and concentration. The nonlinear coupled equations have been solved by a finite element technique with three noded line segments.

The axial velocity (u) is shown in figs1-4 for different values of N , Sc , So and Du . With reference to buoyancy ratio N it can be seen that when the molecular buoyancy force dominates over the thermal buoyancy force, $|u|$ enhances when the buoyancy forces act in same direction and for the forces acting in opposite directions $|u|$ depreciates in the flow region (fig.1). With respect to Schmidt number Sc we find that lesser the molecular diffusivity smaller $|u|$ in the flow region (fig.2). The influence of thermo-diffusion on u is shown in fig3. It can be seen that $|u|$ enhances with increase in So (fig.3). Fig.4 represents with Dufour parameter Du . It can be seen that higher the Dufour effect smaller $|u|$ in the flow region.

The non-dimensional temperature (θ) is shown in figs.5-8 for different parametric values. It is found that the non-dimensional temperature u positive for all variations. This indicates that the actual temperature is greater than T_2 , temperature on $y = 1$. The actual temperature enhances with increase in $N > 0$ and reduces with $|N| (< 0)$ (fig.5). With respect to Sc we find that the actual temperature depreciates with increase in Sc (fig.6). The influence of Soret effect on θ is shown in fig.7. The actual temperature experiences an enhancement with increase in the Soret parameter $|So|$ (fig.7). From fig.8 we find that the actual temperature reduces with increase in $Du \leq 0.7$ and enhances with higher $Du \geq 0.9$.

The concentration distribution (C) is depicted in figs. 9-12 for different parametric values. With reference to buoyancy ratio N we find that the actual temperature enhances with increase in $N > 0$ and depreciates with $|N| (< 0)$ (fig.9). With reference to Sc we notice that the actual concentration enhances with increase in Sc (fig.10). The effect of thermo-diffusion on C is shown in fig.11. It can be seen that the actual concentration reduces with increase in So. From fig.12 we notice that the actual concentration enhances with increase in $Du \leq 0.7$ and reduces with higher $Du \geq 0.9$

The rate of heat transfer (Nusselt number) at the boundaries is shown in tables1-4 for different parametric values. It is found that the rate of heat transfer enhances with increase in $G > 0$ and depreciates with $G < 0$ at both the walls. Higher the Lorentz force, smaller $|Nu|$ for $G > 0$ larger for $G < 0$ at $y = \pm 1$. The variation of Nu with D^{-1} shows that $|Nu|$ depreciates with D^{-1} at $y = +1$ while at $y = -1$, it enhances with $D^{-1} \leq 2 \times 10^2$ and reduces with higher $D^{-1} \geq 3 \times 10^2$ in the heating case and a reversal effect is noticed in $|Nu|$ for $G < 0$. With respect to the buoyancy ratio N, it can be seen that $|Nu|$ enhances in the heating case and reduces in the cooling case at $y = \pm 1$ when the buoyancy forces act in the same direction and for the forces acting in opposite direction, $|Nu|$ reduces for $G > 0$ and enhances for $G < 0$. The variation of Nu with Sc shows that $|Nu|$ reduces with Sc in the heating case and enhances in the cooling case at both the walls (tables1&3). With respect to Soret parameter So we find that $|Nu|$ enhances with increase in $So \leq 1.0$ and for higher $So \geq 1.5$, it reduces for $G > 0$ and enhances for $G < 0$ at $y = \pm 1$. With respect to Duffer parameter Du we find that the rate of heat transfers at $y = +1$, reduces with $Du \leq 0.7$ and enhances with higher $Du \geq 0.9$. At $y = -1$, $|Nu|$ reduces in the heating case and enhances in the cooling case (tables2&4).

The rate of mass transfer (Sherwood number) at $y = \pm 1$ is shown in tables 5-8 for different parametric values. It is found that the rate of mass transfer enhances at $y = +1$ and reduces at $y = -1$ with increase in $G > 0$ while for $G < 0$, $|Sh|$ reduces at $y = +1$ and enhances at $y = -1$. Higher the Lorentz force, lesser $|Sh|$ at $y = +1$ and larger at $y = -1$ in the heating case while in the cooling case, a reversal effect is noticed in the behavior of $|Sh|$. The variation of Sh with D^{-1} shows that $|Sh|$ at $y = +1$ depreciates with $D^{-1} \leq 2 \times 10^2$ and for higher $D^{-1} \geq 3 \times 10^2$, it reduces in the heating case and enhances in the cooling case at $y = -1$, $|Sh|$ reduces for $G > 0$ and enhances for $G < 0$ with increase in $D^{-1} \leq 2 \times 10^2$ while for higher $D^{-1} \geq 3 \times 10^2$, $|Sh|$ enhances for $G > 0$ and reduces for $G < 0$. The variation of Sh with buoyancy ratio N it can be seen that $|Sh|$ enhances at $y = +1$ and reduces at $y = -1$. With increase in $N > 0$ in the heating case while in the cooling case, $|Sh|$ reduces at $y = +1$ and enhances at $y = -1$ when the buoyancy forces act in the same direction and for the forces acting in opposite direction $|Sh|$, reduces at $y = +1$ and enhances at $y = -1$ in the heating case and in the cooling case, it enhances at $y = +1$ and reduces at $y = -1$ with increase in $|N|$. With respect to Sc we find that $|Sh|$ enhances at $y = +1$ and reduces at $y = -1$ for $G > 0$ while in the cooling case it reduces at $y = +1$ and enhances at $y = -1$ with increase in Sc (tables 5&7). An increase in the Soret parameter So reduces $|Sh|$ in the heating case and enhances in the cooling case at both the walls. The variation of Sh with Dufour parameter Du shows that an increase in $Du \leq 0.7$ enhances $|Sh|$ for $G > 0$ and reduces for $G < 0$, while for higher $Du \geq 0.9$, $|Sh|$ reduces for $G > 0$ and enhances for $G < 0$ at $y = +1$. At $y = -1$, $|Sh|$ reduces in the heating case and enhances in the cooling case with increase in Du (tables 6&8).

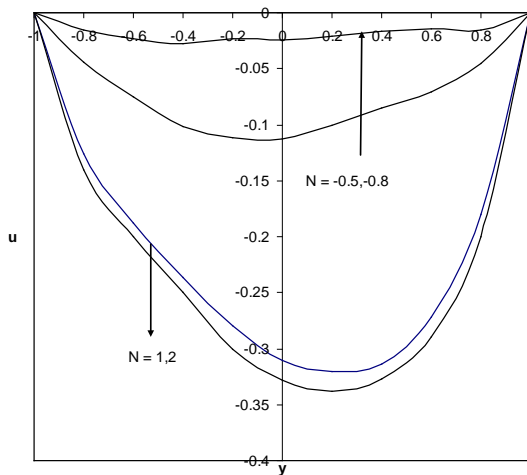


Fig.-1: Variation of u with N, $G = 10^3$, $M = 2$, $G = 10^3$, $M = 2$, $D^{-1} = 10^2$, $Sc = 1.3$, $S_0 = 0.01$, $Du = 0.1$

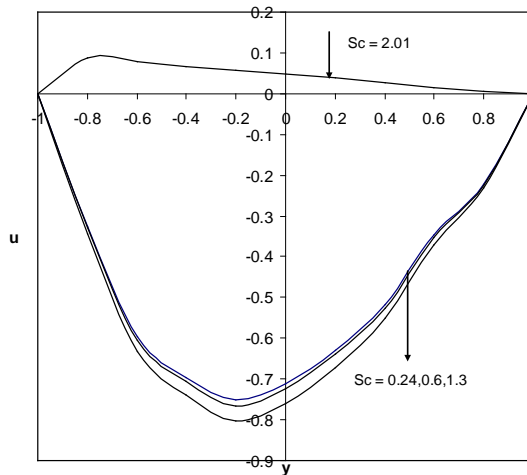


Fig.-2: Variation of u with Sc $G = 10^3$, $M = 2$, $N = 1$, $D^{-1} = 10^2$, $S_0 = 0.01$, $Du = 0.1$

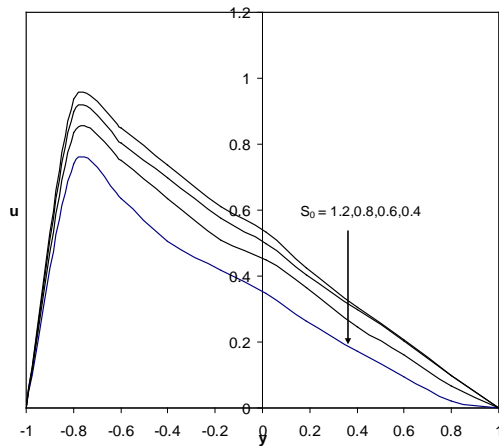


Fig.-3: Variation of u with S_0
 $G = 10^3$, $M = 2$, $N = 1$, $D^{-1} = 10^2$,
 $Sc = 1.3$, $Du = 0.1$

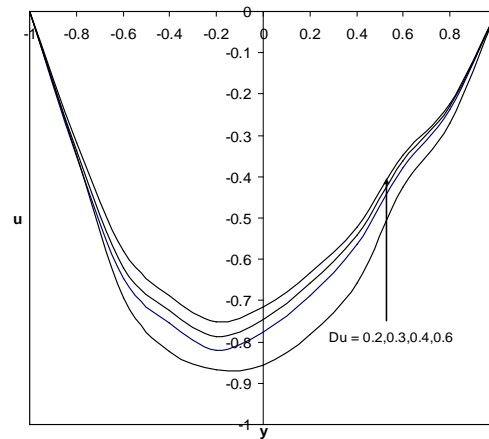


Fig.-4: Variation of u with Du
 $G = 10^3$, $M = 2$, $N = 1$, $D^{-1} = 10^2$
 $Sc = 1.3$, $S_0 = 0.01$

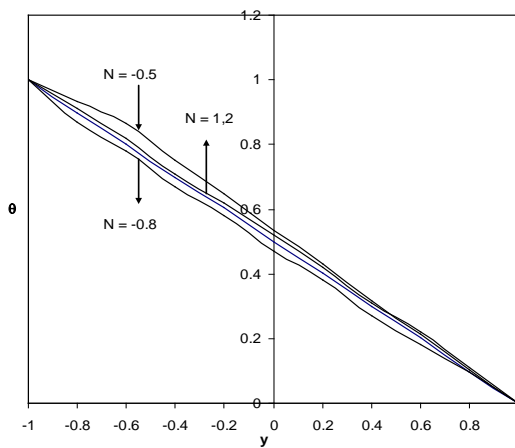


Fig.-5: Variation of θ with N
 $G = 10^3$, $M = 2$, $D^{-1} = 10^2$, $Sc = 1.3$,
 $S_0 = 0.01$, $\gamma = 0.5$, $Du = 0.1$

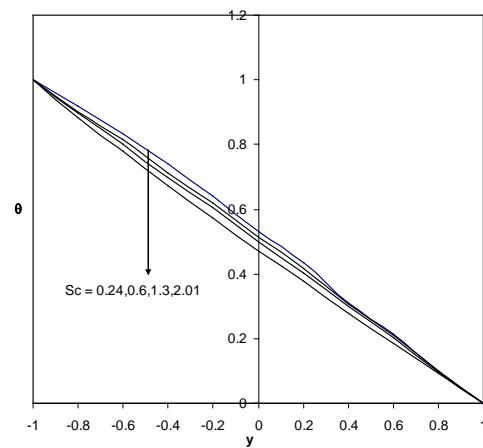


Fig.-6: Variation of θ with Sc
 $G = 10^3$, $M = 2$, $N = 1$, $D^{-1} = 10^2$,
 $S_0 = 0.01$, $\gamma = 0.5$, $Du = 0.1$

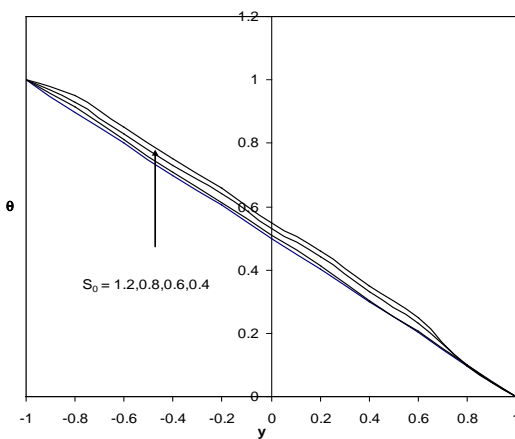


Fig.-7: Variation of θ with S_0
 $G = 10^3$, $M = 2$, $N = 1$, $D^{-1} = 10^2$, $Sc = 1.3$,
 $\gamma = 0.5$, $Du = 0.1$

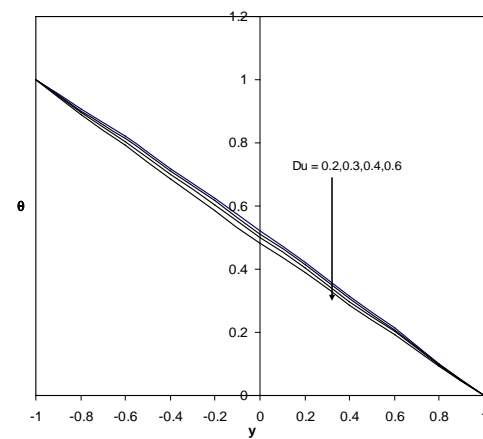


Fig.-8: Variation of θ with Du
 $G = 10^3$, $M = 2$, $N = 1$, $D^{-1} = 10^2$, $Sc = 1.3$,
 $S_0 = 0.01$, $\gamma = 0.5$, $Du = 0.1$

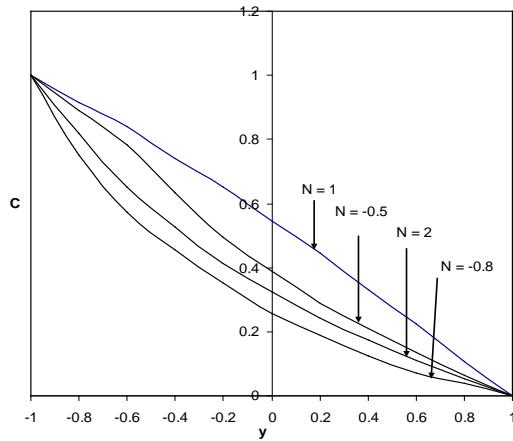


Fig.-9: Variation of C with N
 $G = 10^3$, $M = 2$, $D^{-1}=10^2$, $Sc = 1.3$,
 $S_0 = 0.01$, $\gamma=0.5$, $Du = 0.1$

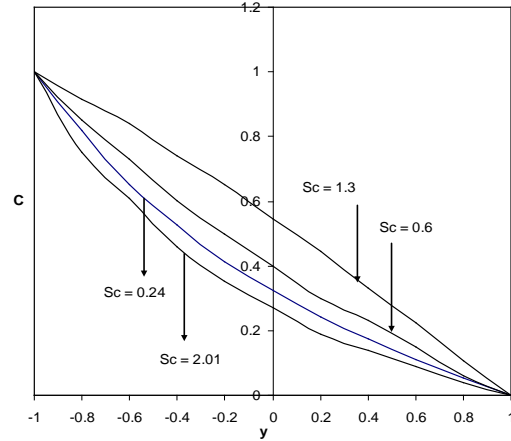


Fig. 10: Variation of C with Sc
 $G = 10^3$, $M = 2$, $N = 1$, $D^{-1}=10^2$,
 $S_0 = 0.01$, $\gamma=0.5$, $Du = 0.1$

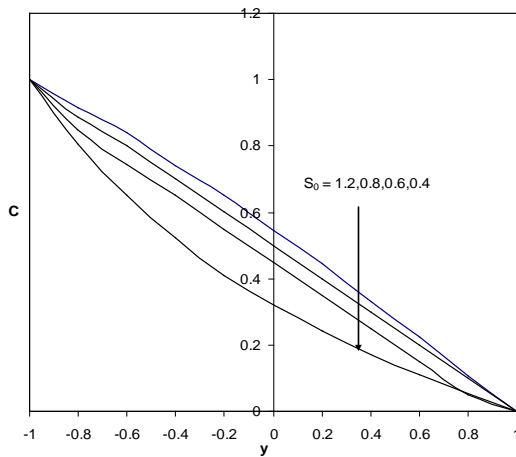


Fig.-11: Variation of C with S_0
 $G = 10^3$, $M = 2$, $N = 1$, $D^{-1}=10^2$, $Sc = 1.3$,
 $\gamma=0.5$, $Du = 0.1$

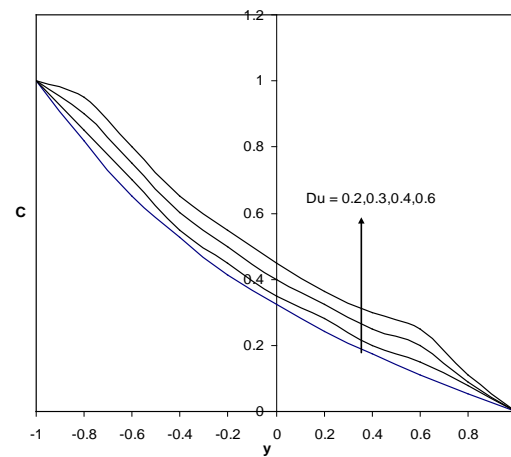


Fig.-12: Variation of C with Du
 $G = 10^3$, $M = 2$, $N = 1$, $D^{-1}=10^2$, $Sc = 1.3$,
 $S_0 = 0.01$, $\gamma=0.5$, $Du = 0.1$

Table-1: Nusselt Number (Nu) at $y = +1$

G	I	II	III	IV	V	VI	VII	VIII	IX	X
10^3	13.9113	13.903	13.9134	13.9242	13.9227	14.3215	13.9061	14.0025	13.9801	13.7962
3×10^3	13.9427	13.9087	13.9531	13.9564	14.2787	14.5333	13.9041	14.2868	14.2155	13.225
-10^3	13.8903	13.8974	13.8887	13.8891	13.8862	13.4733	13.8882	13.8023	13.826	13.9906
-3×10^3	13.8752	13.8932	13.8713	13.8794	12.8456	11.753	13.8411	13.6535	13.7161	14.0909

Annexure-1

M	2	10	2	2	2	2	2	2	2	2
D^{-1}	10^2	10^2	2×10^2	3×10^2	10^2	10^2	10^2	10^2	10^2	10^2
N	1	1	1	1	2	-0.5	-0.8	1	1	1
Sc	1.3	1.3	1.3	1.3	1.3	1.3	1.3	0.24	0.6	2.01

Table-2: Nusselt Number (Nu) at $y = +1$

G	I	II	III	IV	VII	VIII	IX
10^3	13.9113	13.3961	13.9861	13.9861	13.9699	13.8677	13.975
3×10^3	13.9427	13.9583	13.927	13.927	14.2314	13.6613	13.6904
-10^3	13.8903	14.0031	14.0288	14.0228	13.747	13.6786	13.7561
-3×10^3	13.8752	14.0176	14.0431	14.0031	13.563	13.4854	13.8236

Annexure-2

So	0.5	1.0	1.5	2.5	0.5	0.5	0.5
Du	0.5	0.5	0.5	0.5	0.3	0.7	0.9

Table-3: Nusselt Number (Nu) at y = -1

G	I	II	III	IV	V	VI	VII	VIII	IX	X
10 ³	17.1001	17.0249	17.1279	17.1091	17.2328	18.2523	17.0155	18.0279	17.084	15.875
3x10 ³	17.4423	17.0823	17.5533	17.4406	21.6557	18.4995	17.0151	21.053	20.3272	9.3662
-10 ³	16.8267	16.9517	16.8805	16.896	16.8545	15.0021	16.9512	15.9684	16.2186	19.8744
-3x10 ³	16.7489	16.933	16.7124	16.7489	14.18821	7.2593	16.7076	14.476	15.1191	18.864

Annexure-3

M	2	10	2	2	2	2	2	2	2	2
D ⁻¹	10 ²	10 ²	2x10 ²	3x10 ²	10 ²	10 ²	10 ²	10 ²	10 ²	10 ²
N	1	1	1	1	2	-0.5	-0.8	1	1	1
Sc	1.3	1.3	1.3	1.3	1.3	1.3	1.3	0.24	0.6	2.01

Table-4: Nusselt Number (Nu) at y = -1

G	I	II	III	IV	VI	VII	VIII	IX
10 ³	17.1001	17.2371	17.2426	17.2834	18.1131	16.4343	15.9839	15.9839
3x10 ³	17.4423	17.7366	17.7242	17.7546	22.8787	20.5962	14.1517	10.5618
-10 ³	16.8267	16.9634	16.9905	17.0124	16.0498	16.3866	17.5255	18.1135
-3x10 ³	16.7489	16.7663	16.8063	16.8234	14.9004	15.6054	18.0864	19.1696

Annexure-4

So	.50	1.0	1.5	2.5	0.5	0.5	0.5	0.5
Du	0.5	0.5	0.5	0.5	0.1	0.3	0.7	0.9

Table-5: Sherwood Number (Sh) at y = +1

G	I	II	III	IV	V	VI	VII	VIII	IX	X
10 ³	14.0468	13.9342	14.0744	14.0468	14.2986	14.5008	13.9128	13.9271	13.9756	13.9658
3x10 ³	14.4835	14.0117	14.6316	14.4835	17.5535	16.8369	13.9449	14.0017	14.198	14.208
-10 ³	13.7642	13.8648	13.7437	13.7642	13.6497	13.2191	13.8525	13.8746	13.8302	13.8262
-3x10 ³	13.5655	13.8025	13.5233	13.5655	12.6067	10.5356	13.7348	13.8356	13.8366	13.7272

Annexure-5

M	2	10	2	2	2	2	2	2	2	2
D ⁻¹	10 ²	10 ²	2x10 ²	3x10 ²	10 ²	10 ²	10 ²	10 ²	10 ²	10 ²
N	1	1	1	1	2	-0.5	-0.8	1	1	1
Sc	1.3	1.3	1.3	1.3	1.3	1.3	1.3	0.24	0.6	2.01

Table-6: Sherwood Number (Sh) at y = +1

G	I	II	III	IV	V	VI	VII	VII
10 ³	-	14.3827	14.0625	14.0625	14.0588	14.0827	14.1481	14.0526
3x10 ³	-	17.0028	15.0821	15.1821	14.6786	14.7161	15.0313	15.0065
-10 ³	-	13.5278	13.5484	13.5484	13.7692	13.747	13.6786	13.7074
-3x10 ³	-	13.105	13.2401	13.2401	13.6003	13.5452	13.3782	13.5521

Annexure-6

So	0.	1.0	1.5	2.5	0.5	0.5	0.5	0.5
Du	0.5	0.5	0.5	0.5	0.1	0.3	0.7	0.9

Table-7: Sherwood Number (Sh) at y = -1

G	I	II	III	IV	V	VI	VII	VIII	IX	X
10 ³	14.0211	14.0817	14.0063	14.0211	13.8795	13.9943	14.0979	14.0854	14.0594	13.835
3x10 ³	13.773	14.039	13.6869	13.773	11.756	13.9366	14.0795	14.0433	13.933	12.2312
-10 ³	14.1756	14.1165	14.187	14.1756	14.2367	14.2916	14.1266	14.114	14.1388	14.3023
-3x10 ³	14.281	14.145	14.3033	14.281	14.8882	14.9854	14.1805	14.1348	14.1934	14.5195

Annexure-7

M	2	10	2	2	2	2	2	2	2	2
D ⁻¹	10 ⁻²	10 ⁻²	2x10 ⁻²	3x10 ⁻²	10 ⁻²	10 ⁻²	10 ⁻²	10 ⁻²	10 ⁻²	10 ⁻²
N	1	1	1	1	2	-0.5	-0.8	1	1	1
Sc	1.3	1.3	1.3	1.3	1.3	1.3	1.3	0.24	0.6	2.01

Table-8: Sherwood Number (Sh) at y = -1

G	I	II	III	IV	V	VI	VII	VIII	IX
10 ³	13.9882	13.9871	13.908	13.9808	14.0143	14.0015	13.9618	13.9518	13.8624
3x10 ³	13.5257	13.5155	13.4086	13.4475	13.6493	13.6014	13.4516	13.3471	13.3062
-10 ³	14.2298	14.2126	14.3614	14.2387	14.1725	14.1849	14.2264	14.2437	14.2612
-3x10 ³	14.3393	14.344	14.4558	14.3873	14.2606	14.2905	14.3928	14.4272	14.4816

Annexure-8

So	1	1.5	-0.5	-1.0	-1.5	0.5	0.5	0.5	0.5
Du	0.5	0.5	0.5	0.5	0.5	0.1	0.3	0.7	0.9

7. CONCLUSION

In this analysis we discuss the combined influence of thermo-diffusion and diffusion-thermo effects on convective heat and mass transfer flow of a viscous, electrically conducting fluid through a porous medium in a vertical channel whose walls are maintained at constant temperature and concentration. The following conclusions are made in this analysis.

- 1) The axial velocity $|u|$ enhances when the buoyancy forces act in same direction and depreciates for the forces acting in opposite direction. With respect to Schmidt number we find that lesser the molecular diffusivity smaller is the $|u|$ in the flow region. It can be seen that $|u|$ enhances with increase in Soret parameter and depreciates with Dufour parameter.
- 2) The rate of heat transfer (Nusselt number) $|Nu|$ reduces with Sc in heating case and enhances in the cooling case at both the walls.
- 3) The rate of mass transfer (Sherwood number) $|Sh|$, with respect to Soret parameter So, reduces in the heating case and enhances in the cooling case at both the walls.

8. REFERENCES

1. Abdul Sattar,Md. And Alam,Md : Thermal diffusion as well as transprotaion effect on MHD free convection and Mass Transfer flow past an accelerated vertical porous plate , Ind Journal of Pure and Applied Maths.Vol 24,pp.679-688(1995)
2. Ayani,M.B. and Fsfahani,J.H.: The effect of radiation on the natural convection induced by a line heat source.Int.J.Nummer.Method,Heat fluid flow (U.K.),16,28-45(2006)
3. Bharathi, K: Convective heat and mass transfer through a porous medium in channels / pipes with radiation and soret effects, Ph.D. Thesis, S.K.University, Anantapur, A.P., India, (2007)
4. C.Beckermann.R.Visakanta and S.Ramadhyani : A numerical study of non-Darcian natural convection in a vertical enclosure filled with a porous medium., Numerical Heat transfer 10, pp.557-570, (1986).
5. P.Cheng : Heat transfer in geothermal systems., Adv.Heat transfer 14,1-105(1978)
6. El.Hakim,M.A: MHD oscillatory flow on free convection radiation though a porous medium with constant suction velocity ,J.mason.Mater,220,271-276(2000)
7. Jha, B. K. and Singh, A. K.: Astrophys. Space Sci. vol.173, p.251 (1990).
8. Kafousia.N.G. ,Astrophys. Space Sci. vol.173, p.251(1990)
9. Kalidas.N. and Prasad, V: Benard convection in porous media Effects of Darcy and Pransdtl Numbers, Int. Syms. Convection in porous media, non-Darcy effects, proc.25th Nat. Heat Transfer Conf.V.1,pp.593-604 (1988).
10. Kumar. A., Singh,N.P., Singh,A.K., Kumar,H.: MHD free convection flow of a viscous fluid past a porous vertical plate through non-homogeneous porous medium with radiation and temperature gradient dependent heat source in slip glow regime, Ultra Sci.Phys.Sci (India) ,18,39-46(2006)
11. G.Laurait and V.Prasad.: natural convection in a vertical porous cavity a numerical study of Brinkman extended Darcy formulation., J.Heat Transfer.pp.295-320(1987).
12. Makinde,O.D: Free convection flow with thermal radiation and mass transfer pass a moving vertical porous plate, Int.Communs.Heat and Mass transfer (U.K)32.1411-1419(2005)
13. Malasetty.M.S,Gaikwad.S.N: Effect of cross diffusion on double diffusive convection in the presence of horizontal gradient,Int.Journal Eng.Science, Vol.40,PP773-787(2002)
14. Poulikakos D., and Bejan, A.: The Departure from Darcy flow in Nat. Convection in a vertical porous layer, physics fluids V.28, pp.3477-3484 (1985).

15. Prasad, V. and Tuntomo, A.: Inertia Effects on Natural Convection in a vertical porous cavity, numerical Heat Transfer, V.11, pp.295-320 (1987)
16. Prasad, V., F.A., Kulacki and M. Keyhani; "Natural convection in a porous medium" J. Fluid Mech. 150p.89-119 (1985)
17. Raphael, A.: Radiation and free convection flow through a porous medium, Int. Commun. Heat and Mass transfer, 25, 289-295 (1998)
18. Taneja, Rajeev and Jain N.C., Effect of magnetic field on free convection mass transfer flow through porous medium with radiation and variable permeability in slip flow regime., J. Nanopart., 31/32, 69, (2002)
19. D. Tien, C.V. and Hong, J.T.: Natural convection in porous media under non-Darcian and non-uniform permeability conditions, Hemisphere, Washington, D.C. (1985)
20. T.L. Tong and E. Subramanian: A boundary layer analysis for natural convection in porous enclosures: use of the Brinkman-extended Darcy model, Int. J. Heat Mass Transfer, 28, pp.563-571 (1985).
21. Vafai, K., Tien, C.L.: Boundary and Inertia effects on flow and Heat Transfer in Porous Media, Int. J. Heat Mass Transfer, V.24., pp.195-203 (1981).
22. Vafai, K., Thyagaraju, R.: Analysis of flow and heat Transfer at the interface region of a porous medium, Int. J. Heat Mass Trans., V.30pp.1391-1405.

Source of support: Nil, Conflict of interest: None Declared

[Copy right © 2014. This is an Open Access article distributed under the terms of the International Journal of Mathematical Archive (IJMA), which permits unrestricted use, distribution, and reproduction in any medium, provided the original work is properly cited.]